

Original Article

MicroRNA-548q is a novel oncogene and potential prognostic biomarker in human gastric cancer

Jiahua Liu, Xingzhi Ni

Department of General Surgery, Renji Hospital, School of Medicine, Shanghai Jiaotong University, Shanghai, China

Received November 24, 2016; Accepted January 7, 2017; Epub March 1, 2017; Published March 15, 2017

Abstract: Increasing evidence reveals that microRNAs (miRNAs), a class of short noncoding RNAs, are aberrantly expressed in gastric cancer (GC). The purpose of the present study is to dig out potential dysregulated miRNAs that are highly involved in GC development. Firstly, we performed miRNA expression profiling in a large CRC cohort from Gene Expression Ominus (GEO), GSE78091 test series. We identified 43 miRNAs that were differentially expressed. The reliability of miRNA expression profiles was further verified in carcinoma tissues and paired adjacent normal tissues from 93 GC patients using qRT-PCR. We found that the expression of miR-548q, which has not been reported previously in GC, was significantly increased in GC tissues and cell lines. Increased miR-548q expression was closely associated with aggressive clinicopathological variables and poor prognosis of GC patients. Moreover, miR-548q silencing noticeably inhibited proliferation, colony formation, migration and invasion in GC cell lines. Down-regulation of miR-548q also markedly repressed epithelial-mesenchymal transition (EMT) process, which is the major mechanism of cancer metastasis. Accordingly, we herein have delineated the oncogenic role of miR-548q in GC. Our results might provide a miRNA-based target for GC treatment.

Keywords: microRNA, gastric cancer, prognosis, epithelial-mesenchymal transition (EMT)

Introduction

As the second leading cause of cancer-related death throughout the world, gastric cancer (GC) has caused great burden on social economy and health [1]. Although the occurrence rates of GC in some regions are gradually decreasing, such as in Netherland, the clinical epidemiology of GC differs distinctly among various regions [2]. Multiple factors contribute to the prevalence of GC, including unhealthy dietary, irregular lifestyle, and the infection of helicobacter pylori. Age and gender may also affect the morbidity and mortality, and an increasing trend of GC was shown in the 40-54 age-group in South Korean [3]. GC could be categorized into two subgroups, including cardia and non-cardia GC. Data revealed that in 2012, approximately 260,000 cases of cardia GC and 691,000 cases of non-cardia GC occurred globally [4]. The rapid development of GC screening is helpful for patients to receive suitable chemotherapy and surgical resection on early stage [5].

Yoon *et al.* believed that conduction of endoscopic surveillance in atrophic gastritis or intestinal metaplasia patients might aid in the prevention or early detection of GC [6]. However, to date, the effectiveness of GC screening techniques, including upper gastrointestinal endoscopy, remained largely limited [7]. Accumulating studies pay attention to exploring biomarkers to diagnosis GC and to evaluate the prognosis of GC patients [8]. Among multiple biomarkers involved in GC, microRNAs (miRNAs) are considered as potential promising biomarkers with lots of relevant studies [9].

It has been widely documented that miRNAs, a class of endogenous small non-coding RNAs with about 22 nucleotides in length, serve pivotal roles through regulating gene expression posttranscriptionally [10]. Hundreds of miRNAs were found to be aberrantly expressed in carcinoma tissues, and were demonstrated to be implicated in a wide variety of biological processes, such as cell proliferation, apoptosis

Table 1. Correlation between clinicopathological variables and miR-548q expression in a cohort of 93 GC patients

Variables	Total number	miR-548q expression		P value
		Low (n=52)	High (n=41)	
Age (years)				0.723
<60	29	17	12	
≥60	64	35	29	
Gender				0.471
Male	56	33	23	
Female	37	19	18	
Tumor size (cm)				0.060
<5	51	33	18	
≥5	42	19	23	
Location				0.661
Cardia + body	59	34	25	
Pylorus	34	18	16	
Distant metastasis				0.019
Absent	70	44	26	
Present	23	8	15	
Lymph node invasion				0.109
Absent	45	29	16	
Present	48	23	25	
Differentiation status				0.194
Well	12	7	5	
Moderate	36	24	12	
Poor	45	21	24	
TNM stage				0.012
I-II	31	23	8	
III-IV	62	29	33	

and differentiation [11, 12]. For example, miR-21 expression was found to be associated with the aggressive characteristics of GC patients, and up-regulation of miR-21 may promote the proliferation, invasion and migration of GC cells [13]. Zhang *et al.* also indicated that miR-21 could regulate PTEN expression to affect GC cell proliferation and invasion [14]. Moreover, let-7 miRNA family was believed to suppress the metastasis and progression of GC [15-18]. Owing to their abundant and stable expression, miRNAs are considered as potential biomarkers for diagnosing GC, such as miR-199a-3p and miR-106a [19-21]. Among multiple miRNAs, miR-548q has not been fully studied. The article of Zheng *et al.* showed that miR-548q might be one of the promising biomarkers of nasopharyngeal carcinoma (NPC). The NPC patients with poor prognosis tended to exhibit increased miR-548q expression, indicating its

potential prognostic value [22]. Another study showed that miR-548q expression in anal mucosa was evidently reduced among anal fistula patients [23]. However, the function of miR-548q in GC remains elusive.

In the present study, we showed for the first time that miR-548q is significantly increased in GC. The findings might improve our understanding of the molecular mechanisms of GC.

Materials and methods

Study populations

We obtained paired fresh GC and matched adjacent normal tissue specimens from 93 patients who had undergone gastrointestinal surgery at Renji Hospital of Shanghai Jiao Tong University (Shanghai, China). No patient had received adjuvant chemotherapy or radiotherapy prior to surgery. GC and matched histologically normal tissues from each subject were immediately frozen in liquid nitrogen after resection, followed by storage at -80°C. Written informed consent was obtained from all individuals, and the study was approved by the Institutional Review Board of Shanghai Jiao Tong University. The

clinical features of all patients are listed in **Table 1**.

Cell lines

Normal human gastric mucosa cells GES-1 and GC cell lines including AGS, BGC-823, HGC-27, SGC-7901 and MGC-803 were obtained from the Cell Bank of the Chinese Academy of Sciences (Shanghai, China). Cells were maintained in RPMI 1640 medium (Invitrogen, Carlsbad, CA, USA) supplemented with 10% fetal bovine serum (FBS; Invitrogen) in a humidified incubator (Forma Scientific, Marietta, OH, USA) with 5% CO₂ at 37°C.

Choice of differentially expressed long non-coding RNA list using heat map analysis

The microarray data was obtained from Gene Expression Omnibus (GEO; <http://www.ncbi>).

miR-548q promotes GC progression

Table 2. Sequences of qRT-PCR primers

Gene name	Primer sequences
miR-548q-RT	GTCGTATCCAGTGCAGGGTCCGAGGTATTTCGCACTGGATACGACCCGCA
U6-RT	GTCGTATCCAGTGCAGGGTCCGAGGTATTTCGCACTGGATACGACAAAATA
miR-548q Forward primer	CTGCTGGTGCAAAAGTAA
miR-548q Reverse primer	GTGCAGGGTCCGAGGT
U6 Forward primer	CTCGCTTCGGCAGCACATATACT
U6 Reverse primer	ACGCTTCACGAATTTGCGTGTCT

nlm.nih.gov/geo/), and the GEO accession number is GSE78091. The data was generated using the platform miRCURY LNA microRNA Array, 7th generation-hsa, MMU & RNO (miR-Base 21; probelD version).

Observations with adjusted *P* values ≥ 0.05 were removed and thus excluded from further analysis. In the heat map of the 43 miRNAs, most obvious differences was created using a method of hierarchical clustering by GeneSpring GX, version 7.3 (Agilent Technologies, CA, USA).

Total RNA extraction and qRT-PCR analysis

Total RNA was isolated from tissues and cells using RNAiso Plus (Takara, Dalian, China). RNA was determined at a 260/280 nm wavelength ratio measured by a NanoDrop spectrometer (Thermo Scientific, Waltham, MA, USA). 1 μ g of total RNA was reverse-transcribed into cDNA using the All-in-One™ miRNA Q-PCR Detection Kit (Genecopoeia, Germantown, MD, USA). After the reverse transcription, 0.5 μ l of the cDNA was used for subsequent quantitative real-time PCR (qRT-PCR). qRT-PCR was conducted using the SYBR-Green Master Mix (Applied Biosystems, Foster City, CA, USA) on ABI PRISM 7000 Fluorescent Quantitative PCR System (Applied Biosystems). U6 small nuclear RNA was used as an endogenous control. The qRT-PCR primers were synthesized by Sangon Biotech, Co., Ltd. (Shanghai, China). Their sequences were recorded in **Table 2**. The relative quantitative value was expressed by the $2^{-\Delta\Delta Ct}$ method [24]. Independent experiments were done in triplicate.

Transfection

MiR-548q inhibitor (anti-miR-548q) and miR-548q inhibitor negative control (anti-miR-NC) were designed and synthesized by RiboBio (Ribobio Co., Guangzhou, China). For transfection,

cells were seeded in 6-well plates at a density of 1×10^5 cells/well and transfected with 20 μ M anti-miR-548q or anti-miR-NC using Lipofectamine™ 2000 (Invitrogen, Carlsbad, CA, USA) following the manufacturer's instruction.

CCK-8 assay

Cell proliferation was measured using the Cell Counting Kit 8 (CCK-8; Dojin Laboratories, Kumamoto, Japan). Briefly, AGS or SGC-7901 cells were seeded into a 96-well plate at a density of 1000 cells per well. At various time points (0, 24, 48, 72, and 96 h), 10 μ L of CCK-8 reagent was added to each well. The optical density (OD) value was detected at a wavelength of 450 nm using a microplate reader (Bio-Rad, Hercules, CA, USA). Three independent experiments (three replicates in each) were performed.

Colony formation assay

1000 transfected AGS or SGC-7901 cells were grown in each well of a 12-well plate and allowed to grow for 12 days in RPMI-1640 containing 10% FBS. Colonies were fixed with methanol and then stained with 0.1% crystal violet solution, and the number of macroscopically observable colonies was counted under a microscope.

Apoptosis assay

Cell apoptosis was investigated according to the instructions provided in an Annexin V-FITC and PI double-stain detection kit (Key Gen Biotech, Nanjing, China). Briefly, after transfection, AGS or SGC-7901 cells were harvested and resuspended in binding buffer at a density of 1×10^6 cells/mL. Cells were then stained with Annexin V-FITC and PI in the dark for 15 min at room temperature, followed by cell apoptosis

miR-548q promotes GC progression

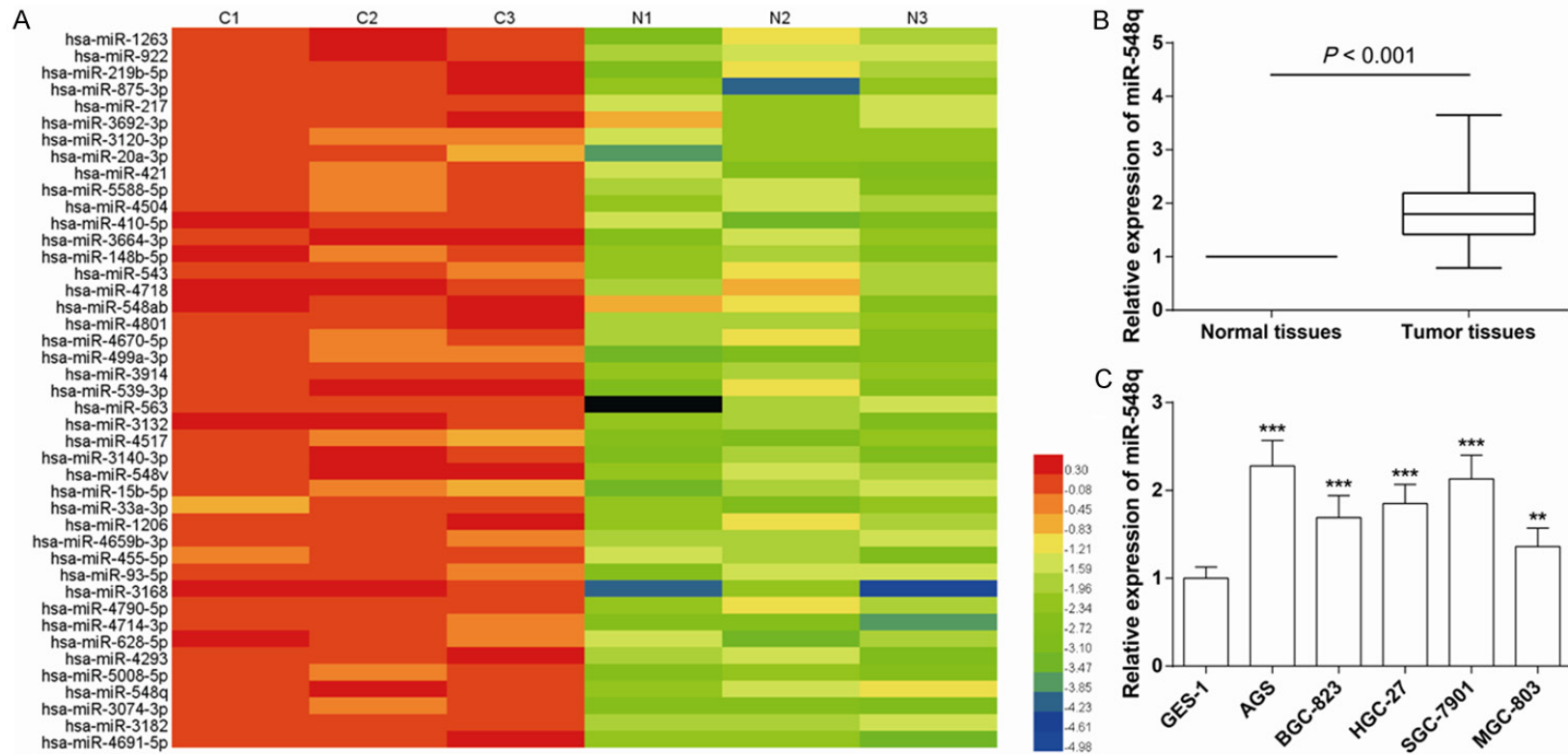


Figure 1. Expression of miR-548q was increased in both GC tissues and cell lines. A: Hierarchical clustering analysis of 43 miRNAs that were differentially expressed between GC tissues and non-tumor samples. For each miRNA, the red color indicates genes with high expression, and the green color denotes genes with low expression. B: Relative miR-548q levels in GC tissues and adjacent non-tumor tissues were detected by qRT-PCR. U6 was used as an internal control. C: Relative miR-548q levels in GC cell lines (AGS, BGC-823, HGC-27, SGC-7901 and MGC-803) and normal gastric mucosa cells line GES-1 were detected by qRT-PCR. U6 levels were used as an internal control. The results represent data from at least three independent experiments presented as mean \pm SD. Student's *t*-test was used with *** $P < 0.001$, ** $P < 0.01$ vs. control.

miR-548q promotes GC progression

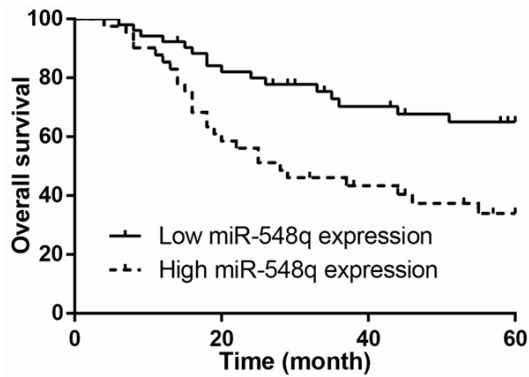


Figure 2. Relationship between miR-548q expression and 5-year overall survival rates of 93 GC patients. *P* value was assessed by log-rank test.

analysis using the FACS Calibur Flow Cytometer (BD, USA). The experiments were repeated in triplicate.

Wound healing assay

Approximately 5×10^4 AGS or SGC-7901 cells were plated in each well of a 6-well plate. When cell confluence reached about 90% after transfection, wounds were manually created in confluent cells using a 200 μ l pipette tip. The cells were rinsed several times with media to remove any free-floating cells and debris. Wound healing was observed at different time points (0, 24, and 48 h) within the scrape line, and representative scrape lines for each cell type were photographed using phase-contrast microscope (Olympus, Japan).

Transwell assay

To detect cell migration and invasion *in vitro*, 1×10^5 AGS or SGC-7901 cells were harvested and resuspended in serum-free RPMI-1640 medium, and cells were placed into the upper chamber of an insert (8 μ m pore size; Millipore, Billerica, MA) coated with (for invasion) or without (for migration) Matrigel (BD Bioscience, USA). The chambers were then inserted into the wells of a 24-well plate and incubated for 48 h in RPMI-1640 medium with 10% FBS before examination. After incubation, cells remained on the upper membrane surface were removed with a cotton tip, and the cells that passed through the filter were fixed with 4% paraformaldehyde and stained with 0.1% crystal violet. Numbers of invaded cells were counted and compared in five randomly selected fields under a microscope.

Total protein extraction and western blot analysis

Total protein from cells was lysed using RIPA lysis buffer (Beyotime, Beijing, China) supplemented with a protease inhibitor cocktail (Sigma, St Louis, MO, USA). Equal amounts of protein were subjected to sodium dodecyl sulfate-polyacrylamide gel electrophoresis (SDS-PAGE), and then transferred to nitrocellulose membrane (Millipore, Bedford, MA). After blocking with 5% non-fat milk in TBST for 60 min, membranes were incubated with primary antibody dissolved in 5% bovine serum albumin in TBST overnight at 4°C. The following primary antibodies were used: anti-human-E-cadherin (1:2000; Cell Signaling Technology, Danvers, MA, USA), anti-human-Vimentin (1:2000; Cell Signaling Technology), anti-human-Snail (1:1000; Cell Signaling Technology), and anti-human-N-cadherin (1:2000; Cell Signaling Technology). Human GAPDH (1:5000; Kang-Chen, Shanghai, China) was used as an internal reference. The membranes were then incubated with corresponding HRP-conjugated secondary antibodies. The blots were later visualized using Image J software (NIH, Bethesda, MD, USA).

Statistical analysis

Statistical analyses were conducted using SPSS 13.0 software (Chicago, Ill., USA) and GraphPad Prism 6.0 (GraphPad Software Inc., CA, USA). Two-tailed Student's *t* test was used for comparisons of two independent groups. The chi-square test was used to the examination of relationship between miR-548q expression levels and clinicopathologic characteristics of GC patients. Overall survival (OS) time was calculated from the date of the initial surgical operation to death. Survival curves were plotted using the Kaplan-Meier method and the log-rank test. The significance of survival variables was analyzed using the Cox multivariate proportional hazards model. For all tests, a *P*-value of <0.05 was regarded statistically significant.

Results

miR-548q is highly expressed in GC tissues and cell lines

Initially, hierarchical clustering demonstrated differentially expressed miRNAs between GC

miR-548q promotes GC progression

Table 3. Univariate analysis of potential prognostic factors in 93 GC patients

Characteristics	Univariate analysis		
	Risk ratio	95% CI	P value
Age (years)			
<60 vs. ≥60	0.452	0.185-1.106	0.082
Gender			
Male vs. Female	0.811	0.352-1.867	0.623
Tumor size (cm)			
<5 vs. ≥5	2.444	1.057-5.654	0.037
Location			
Cardia + body vs. Pylorus	1.983	0.843-4.665	0.117
Distant metastasis			
Absent vs. Present	2.986	1.116-7.987	0.029
Lymph node invasion			
Absent vs. Present	2.142	0.931-4.930	0.073
Differentiation status			
Well vs. Moderate/Poor	1.905	0.833-4.357	0.127
TNM stage			
I-II vs. III-IV	5.769	2.072-16.062	0.001
miR-548q expression			
Low vs. High	3.900	1.640-9.275	0.002

Table 4. Multivariate analysis of potential prognostic factors in 93 GC patients

Characteristics	Multivariate analysis		
	Risk ratio	95% CI	P value
Tumor size (cm)			
<5 vs. ≥5	1.404	0.535-3.683	0.490
Distant metastasis			
Absent vs. Present	2.164	0.726-6.454	0.166
TNM stage			
I-II vs. III-IV	4.040	1.330-12.267	0.014
miR-548q expression			
Low vs. High	2.638	1.030-6.756	0.043

and paired non-tumor tissues (**Figure 1A**), and miR-548q, which has not been previously reported in GC, was accordingly speculated as a novel oncogene in GC. In order to further validate the expression pattern of miR-548q in GC, we performed qRT-PCR to detect the expression of miR-548q in 93 clinical fresh samples of GC tissues and adjacent non-cancerous tissues. As shown in **Figure 1B**, compared with adjacent non-cancerous tissues, GC tissues showed significantly increased expression levels of miR-548q ($P < 0.001$).

Next, we performed qRT-PCR to evaluate the levels of miR-548q in five GC cell lines and one

normal human gastric mucosa cell line (GES-1). The expression of miR-548q was overexpressed in all five GC cell lines compared with the levels observed in GES-1 cells, with the highest in AGS cells (**Figure 1C**).

Relationship between clinicopathological characteristics and miR-548q expression in GC patients

We further determined the association between the expression of miR-548q and clinicopathological characteristics of GC patients. GC tissue samples were classified into the low expression group (n=52) and the high expression group (n=41) according to the median expression level of miR-548q in all GC samples. The association between clinicopathological characteristics and miR-548q expression levels in GC patients was summarized in **Table 1**. We did not observe any significant correlation of miR-548q expression levels with patient's age ($P=0.723$), gender ($P=0.471$), tumor size ($P=0.060$), location ($P=0.661$), lymph node invasion ($P=0.109$) and differentiation status ($P=0.194$). However, miR-548q expression was positively associated with distant metastasis ($P=0.019$) and TNM stage ($P=0.012$) in GC patients.

miR-548q expression is associated with overall survival of GC patients

To explore the prognostic value of miR-548q expression for GC, we assessed the association between the levels of miR-548q expression and GC patients' overall survival through Kaplan-Meier analysis and log-rank test. In 93 GC patients, we found that miR-548q expression was closely associated with GC patients' overall survival ($P=0.003$, **Figure 2**). In other words, patients with higher miR-548q expression had worse overall survival than those with lower expression of miR-548q.

Furthermore, univariate analysis demonstrated that tumor size, distant metastasis, TNM stage and miR-548q expression were significantly correlated with unfavorable overall survival of GC patients (**Table 3**). Multivariate analysis revealed that relative miR-548q expression level and TNM stage were independent prog-

miR-548q promotes GC progression

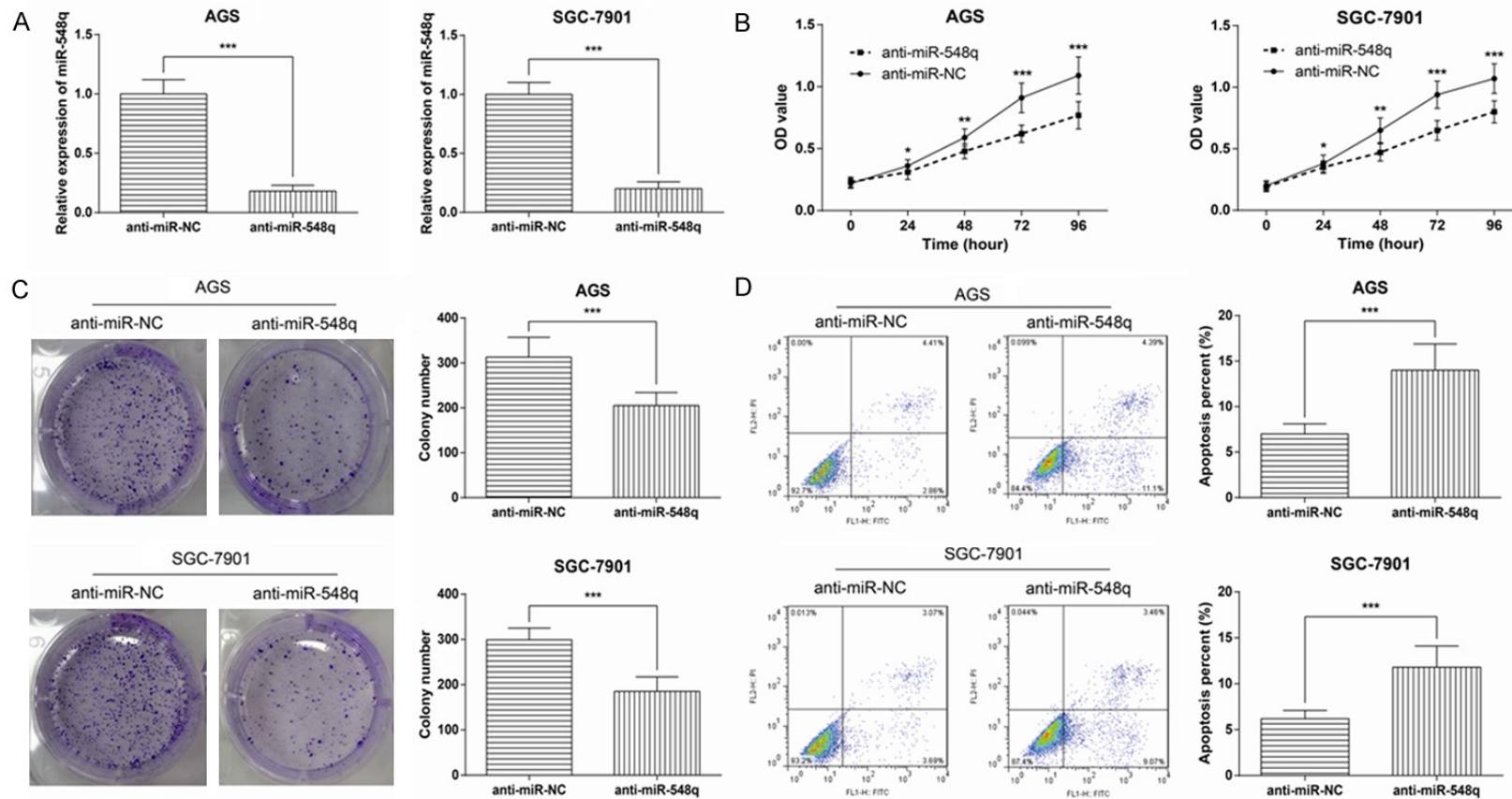
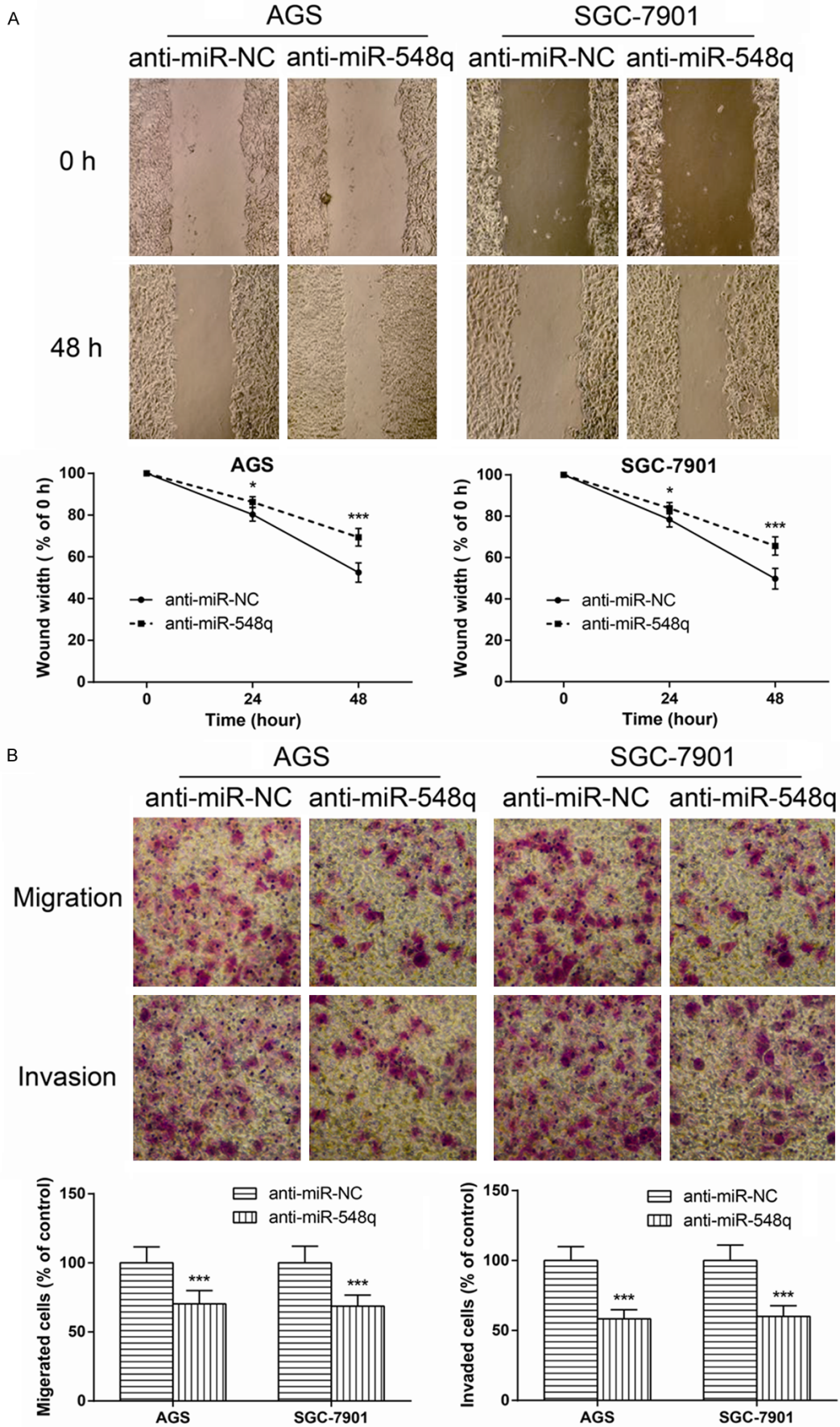


Figure 3. miR-548q expression promotes proliferation of GC cells and inhibits apoptosis of GC cells. A: qRT-PCR analysis was performed to evaluate the transfection efficiency in AGS and SGC-7901 cells after transfection with anti-miR-548q. B: Proliferation of AGS and SGC-7901 cells transfected with anti-miR-548q was investigated by CCK-8 assay at the indicated time points. C: Colony formation ability of AGS and SGC-7901 cells transfected with anti-miR-548q was evaluated. D: Apoptosis rates were determined by flow cytometric analysis in AGS and SGC-7901 cells transfected with anti-miR-548q. The results represent data from at least three independent experiments presented as mean \pm SD. Student's *t*-test was used with *** P <0.001, ** P <0.01, * P <0.05 vs. control.

miR-548q promotes GC progression



miR-548q promotes GC progression

Figure 4. miR-548q promotes GC cells migration and invasion. A: Wound healing assay was performed to detect the motility in AGS and SGC-7901 cells transfected with anti-miR-548q. Images were captured at 0 h, 24 h and 48 h post-wounding. B: Transwell assay was employed to examine the migratory and invasive capacities in AGS and SGC-7901 cells transfected with anti-miR-548q. Representative images of migrated and invaded cells at the bottom of the membrane stained with crystal violet are shown. The results represent data from at least three independent experiments presented as mean \pm SD. Student's *t*-test was used with *** P <0.001, * P <0.05 vs. control.

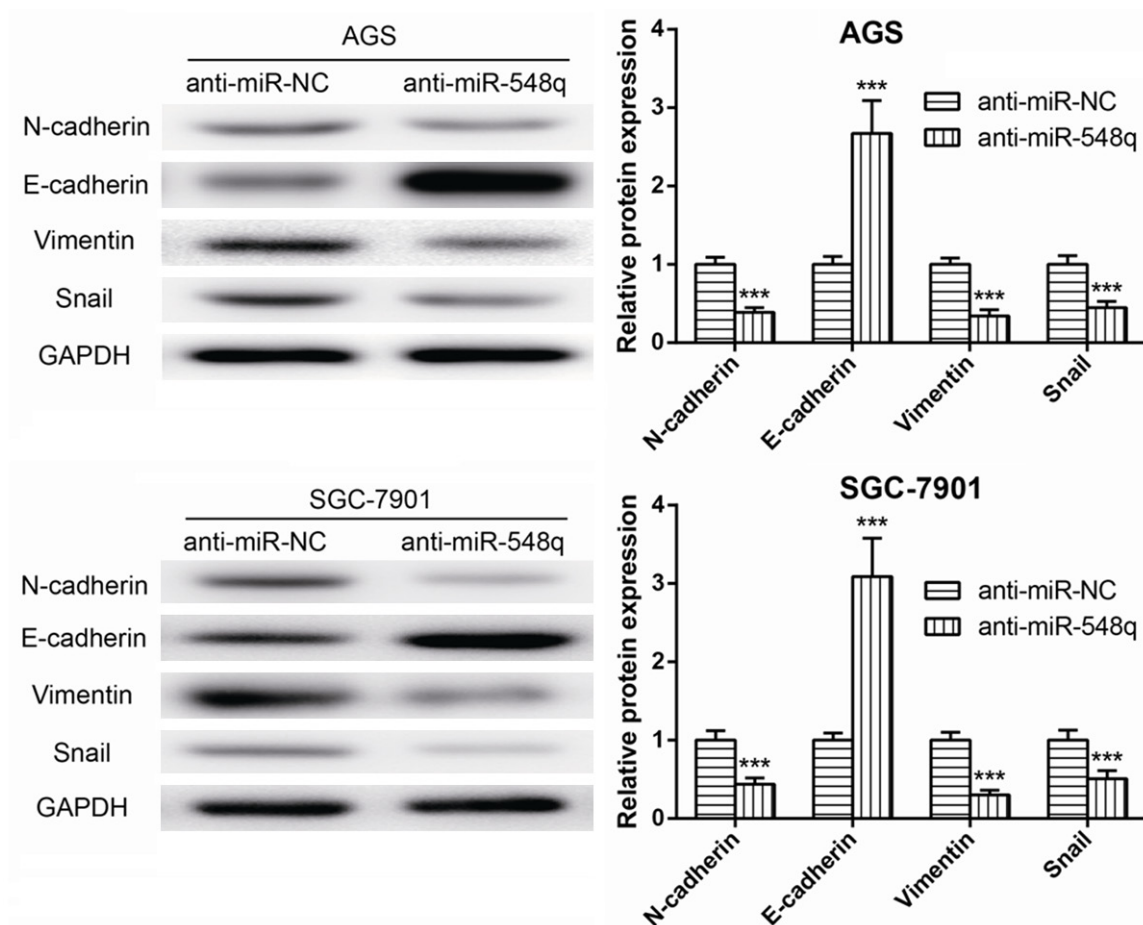


Figure 5. miR-548q induces epithelial-mesenchymal transition (EMT) in GC. Levels of EMT markers, including E-cadherin, N-cadherin, Vimentin and Snail, were detected by western blot analysis when miR-548q is down-regulated in AGS and SGC-7901 cells. GAPDH levels were used as a loading control. The results represent data from at least three independent experiments presented as mean \pm SD. Student's *t*-test was used with *** P <0.001 vs. control.

nostic indicators for the overall survival of GC patients (Table 4). These results revealed that miR-548q expression could be considered as a powerful independent factor for predicting the prognosis of GC patients.

miR-548q expression promotes proliferation of GC cells and inhibits apoptosis of GC cells

To identify the biological roles of miR-548q on GC cells, we transfected 2 GC cell lines: AGS and SGC-7901 with anti-miR-NC and anti-miR-548q, respectively. The transfection efficiency

was confirmed by qRT-PCR in GC cells (Figure 3A). Next, we examined the effect of decreased miR-548q expression on GC cell growth *in vitro*. The growth curves determined by CCK-8 assay exhibited that AGS and SGC-7901 cells transfected with anti-miR-548q had a decreased growth rate compared with controls at 48, 72 and 96 hours after transfection (Figure 3B). The results of colony formation assay were also consistent with CCK-8 assay as AGS and SGC-7901 cells transfected with anti-miR-548q formed a decreased number of colonies compared to controls over a 12-day period (Figure

3C). This suggested that miR-548q knockdown dramatically suppress proliferation of GC cells.

To further elucidate the mechanism of miR-548q-mediated cell proliferation in GC cells, apoptosis analysis was also performed. Results showed that apoptosis rates increased in AGS and SGC-7901 cells transfected with anti-miR-548q compared with that in the controls, indicating that miR-548q suppressed the apoptosis of GC cells (**Figure 3D**).

miR-548q promotes GC cells migration and invasion

Wound healing and transwell assays were performed to investigate the effects of miR-548q on the migration and invasion of GC cells. As shown in **Figure 4A**, compared to controls, AGS and SGC-7901 cells migrated the shorter distance following the transfection of anti-miR-548q. Also, transwell assay showed that, the migratory and invasive capacities of AGS and SGC-7901 cells transfected with anti-miR-548q were remarkably suppressed compared with controls (**Figure 4B**).

miR-548q induces epithelial-mesenchymal transition (EMT) in GC

EMT is a main mechanism involved in cell migration and invasion. Accordingly, we next explored the expression of EMT-associated proteins in GC cells after transfection. The expression levels of E-cadherin, N-cadherin, Vimentin and Snail were investigated by Western blot. By data, we observed that the levels of N-cadherin, Vimentin and Snail were obviously decreased, while E-cadherin expression was markedly boosted when miR-548q was knocked down in AGS and SGC-7901 cells (**Figure 5**). These data suggested that miR-548q involves mechanisms relevant to the promotion of GC cell migration and invasion and that the underlying mechanisms may function through regulating the EMT pathway.

Discussion

GC is a prevailing malignancy with high morbidity and mortality; hence, it is in urgent required to find effective therapeutic methods for GC. Better understanding the mechanisms of GC could contribute to effective diagnosis and treatment of GC, with a prediction model for GC

incidence in South Korean showing ideal accuracy [25]. In renal cell carcinoma, miR-548q could control the immune effector cell activity through contributing to an enhanced NK cell-mediated HLA-G-dependent cytotoxicity [26]. However, the function of miR-548q in GC has not been well studied previously.

In this study, miR-548q expression in GC tissues was significantly elevated compared to that in control samples. The expression levels of miR-548q in five GC cell lines were also higher than that in normal human gastric mucosa cell line. Furthermore, we analyzed the expression of miR-548q with clinical features of 93 patients, indicating the distant metastasis and advanced TNM stage in GC patients were positively associated with miR-548q expression. Moreover, miR-548q expression was closely associated with GC patients' overall survival by Kaplan-Meier analysis and log-rank test, and the patients with relative high miR-548q expression tended to have poor prognosis, indicating miR-548q might serve as a potential prognosis biomarker for GC. A wide variety of dysregulated miRNAs are found to be associated with the prognostic outcomes of GC patients, such as abnormal expression of miR-125b, overexpression of miR-196b, and down-regulation of miR-326 [27-29]. Whether miR-548q could be used in combination with these miRNAs for evaluating the prognosis of GC patients was required to be further studied.

The above research revealed the correlation between miR-548q and GC, and then we conducted *in vitro* functional assays to investigate the role of miR-548q in GC. CCK-8 assay showed that the GC cells transfected with anti-miR-548q had a significantly decreased growth rate than control cells, suggesting miR-548q may promote the proliferation of GC cells. Moreover, the increased apoptosis rates in GC cells transfected with anti-miR-548q indicated that miR-548q could mediate the apoptosis of GC cells. Due to the association between miR-548q and distant metastasis in GC patients, the wound healing and transwell assays were thus conducted. The results showed that the migratory and invasive capacities of cells transfected with anti-miR-548q remarkably reduced, indicating miR-548q could effectively enhance GC cell migration and invasion. Mounting evidences have shown that EMT process partici-

pates in the onset of metastasis in GC [30, 31]. Herein, a series of EMT-related proteins, including N-cadherin, Vimentin and Snail, expressed significantly lower while E-cadherin expression increased remarkably when miR-548q silenced in GC cells, indicating that miR-548q participates in the metastasis of GC cells partly through mediating EMT process. From our research, miR-548q could be considered as a critical factor promoting GC progression. Previous studies showed that, in breast cancer, miR-548-3p functioned as an anti-oncogenic regulator through inhibiting the proliferation of tumor cells [32]. Ke *et al.* found that overexpressing miR-548ar reduces NEAT1 expression to induce apoptosis in breast cancer cells [33]. The different functions of these miRNAs might be correlated with the diverse expression profiles of miR-548 family in different human tissues.

Although the data in our research are compelling, there are still a number of limitations should be noted. Down-regulation of miR-548q could effectively suppress the proliferation and metastasis of GC cells, while the promotion on cell growth and migration needed be confirmed by up-regulating miR-548q expression in normal gastric mucosa cells to observe corresponding consequences. Besides, we should perform *in vivo* study to investigate whether miR-548q still functions in animal models. Moreover, the target gene interacting with miR-548q is required for better understanding how miR-548q regulates the proliferation and migration of GC cells.

Collectively, it might be the first time to indentify the role of miR-548q in GC, which promotes GC cell proliferation, inhibit cell apoptosis and contribute to EMT process. MiR-548q exhibited its potential function as a therapeutic target or prognosis biomarker for GC.

Acknowledgements

The work of our research was supported by National Natural Science Foundation of China (No. 81302094).

Disclosure of conflict of interest

None.

Address correspondence to: Xingzhi Ni, Department of General Surgery, Renji Hospital, School of

Medicine, Shanghai Jiaotong University, Shanghai 200127, China. E-mail: georgeniwjc@sina.com

References

- [1] Ang TL and Fock KM. Clinical epidemiology of gastric cancer. *Singapore Med J* 2014; 55: 621-628.
- [2] Dassen AE, Dikken JL, Bosscha K, Wouters MW, Cats A, van de Velde CJ, Coebergh JW and Lemmens VE. Gastric cancer: decreasing incidence but stable survival in the Netherlands. *Acta Oncol* 2014; 53: 138-142.
- [3] Song M, Kang D, Yang JJ, Choi JY, Sung H, Lee Y, Yoon HS, Choi Y, Kong SH, Lee HJ, Yang HK and Kim WH. Age and sex interactions in gastric cancer incidence and mortality trends in Korea. *Gastric Cancer* 2015; 18: 580-589.
- [4] Colquhoun A, Arnold M, Ferlay J, Goodman KJ, Forman D and Soerjomataram I. Global patterns of cardia and non-cardia gastric cancer incidence in 2012. *Gut* 2015; 64: 1881-1888.
- [5] Barreto SG and Windsor JA. Redefining early gastric cancer. *Surg Endosc* 2016; 30: 24-37.
- [6] Yoon H and Kim N. Diagnosis and management of high risk group for gastric cancer. *Gut Liver* 2015; 9: 5-17.
- [7] Hamashima C. Current issues and future perspectives of gastric cancer screening. *World J Gastroenterol* 2014; 20: 13767-13774.
- [8] Aichler M, Luber B, Lordick F and Walch A. Proteomic and metabolic prediction of response to therapy in gastric cancer. *World J Gastroenterol* 2014; 20: 13648-13657.
- [9] Liu HS and Xiao HS. MicroRNAs as potential biomarkers for gastric cancer. *World J Gastroenterol* 2014; 20: 12007-12017.
- [10] Gibson NW. Engineered microRNA therapeutics. *J R Coll Physicians Edinb* 2014; 44: 196-200.
- [11] Mohr AM and Mott JL. Overview of microRNA biology. *Semin Liver Dis* 2015; 35: 3-11.
- [12] Simonson B and Das S. MicroRNA therapeutics: the next magic bullet? *Mini Rev Med Chem* 2015; 15: 467-474.
- [13] Sun H, Wang P, Zhang Q, He X, Zai G, Wang X, Ma M and Sun X. MicroRNA21 expression is associated with the clinical features of patients with gastric carcinoma and affects the proliferation, invasion and migration of gastric cancer cells by regulating Noxa. *Mol Med Rep* 2016; 13: 2701-2707.
- [14] Zhang BG, Li JF, Yu BQ, Zhu ZG, Liu BY and Yan M. microRNA-21 promotes tumor proliferation and invasion in gastric cancer by targeting PTEN. *Oncol Rep* 2012; 27: 1019-1026.
- [15] Ohshima K, Inoue K, Fujiwara A, Hatakeyama K, Kanto K, Watanabe Y, Muramatsu K, Fukuda Y, Ogura S, Yamaguchi K and Mochizuki T.

miR-548q promotes GC progression

- Let-7 microRNA family is selectively secreted into the extracellular environment via exosomes in a metastatic gastric cancer cell line. *PLoS One* 2010; 5: e13247.
- [16] Liu WJ, Xu Q, Sun LP, Dong QG, He CY and Yuan Y. Expression of serum let-7c, let-7i, and let-7f microRNA with its target gene, pepsinogen C, in gastric cancer and precancerous disease. *Tumour Biol* 2015; 36: 3337-3343.
- [17] Hu H, Zhao X, Jin Z and Hou M. Hsa-let-7g miRNA regulates the anti-tumor effects of gastric cancer cells under oxidative stress through the expression of DDR genes. *J Toxicol Sci* 2015; 40: 329-338.
- [18] Liang S, He L, Zhao X, Miao Y, Gu Y, Guo C, Xue Z, Dou W, Hu F, Wu K, Nie Y and Fan D. MicroRNA let-7f inhibits tumor invasion and metastasis by targeting MYH9 in human gastric cancer. *PLoS One* 2011; 6: e18409.
- [19] Li C, Li JF, Cai Q, Qiu QQ, Yan M, Liu BY and Zhu ZG. miRNA-199a-3p in plasma as a potential diagnostic biomarker for gastric cancer. *Ann Surg Oncol* 2013; 20 Suppl 3: S397-405.
- [20] Hou X, Zhang M and Qiao H. Diagnostic significance of miR-106a in gastric cancer. *Int J Clin Exp Pathol* 2015; 8: 13096-13101.
- [21] Shin VY, Ng EK, Chan VW, Kwong A and Chu KM. A three-miRNA signature as promising non-invasive diagnostic marker for gastric cancer. *Mol Cancer* 2015; 14: 202.
- [22] Zheng XH, Cui C, Ruan HL, Xue WQ, Zhang SD, Hu YZ, Zhou XX and Jia WH. Plasma microRNA profiling in nasopharyngeal carcinoma patients reveals miR-548q and miR-483-5p as potential biomarkers. *Chin J Cancer* 2014; 33: 330-338.
- [23] Qiu J, Yu J, Yang G, Xu K, Tao Y, Lin A and Wang D. [Detection and analysis of the characteristic expression of microRNAs of anal fistula patients]. *Zhonghua Wei Chang Wai Ke Za Zhi* 2016; 19: 789-792.
- [24] Livak KJ and Schmittgen TD. Analysis of relative gene expression data using real-time quantitative PCR and the 2⁻(Delta Delta C(T)) Method. *Methods* 2001; 25: 402-408.
- [25] Eom BW, Joo J, Kim S, Shin A, Yang HR, Park J, Choi IJ, Kim YW, Kim J and Nam BH. Prediction model for gastric cancer incidence in Korean population. *PLoS One* 2015; 10: e0132613.
- [26] Jasinski-Bergner S, Reches A, Stoehr C, Massa C, Gonschorek E, Huettelmaier S, Braun J, Wach S, Wullich B, Spath V, Wang E, Marincola FM, Mandelboim O, Hartmann A and Seliger B. Identification of novel microRNAs regulating HLA-G expression and investigating their clinical relevance in renal cell carcinoma. *Oncotarget* 2016; 7: 26866-26878.
- [27] Wu JG, Wang JJ, Jiang X, Lan JP, He XJ, Wang HJ, Ma YY, Xia YJ, Ru GQ, Ma J, Zhao ZS and Zhou R. MiR-125b promotes cell migration and invasion by targeting PPP1CA-Rb signal pathways in gastric cancer, resulting in a poor prognosis. *Gastric Cancer* 2015; 18: 729-739.
- [28] Lim JY, Yoon SO, Seol SY, Hong SW, Kim JW, Choi SH, Lee JS and Cho JY. Overexpression of miR-196b and HOXA10 characterize a poor-prognosis gastric cancer subtype. *World J Gastroenterol* 2013; 19: 7078-7088.
- [29] Xu XD, He XJ, Tao HQ, Zhang W, Wang YY, Ye ZY and Zhao ZS. Abnormal expression of miR-301a in gastric cancer associated with progression and poor prognosis. *J Surg Oncol* 2013; 108: 197-202.
- [30] Xu SH, Huang JZ, Xu ML, Yu G, Yin XF, Chen D and Yan GR. ACK1 promotes gastric cancer epithelial-mesenchymal transition and metastasis through AKT-POU2F1-ECD signalling. *J Pathol* 2015; 236: 175-185.
- [31] Liu YW, Sun M, Xia R, Zhang EB, Liu XH, Zhang ZH, Xu TP, De W, Liu BR and Wang ZX. LinchOTAIR epigenetically silences miR34a by binding to PRC2 to promote the epithelial-to-mesenchymal transition in human gastric cancer. *Cell Death Dis* 2015; 6: e1802.
- [32] Shi Y, Qiu M, Wu Y and Hai L. MiR-548-3p functions as an anti-oncogenic regulator in breast cancer. *Biomed Pharmacother* 2015; 75: 111-116.
- [33] Ke H, Zhao L, Feng X, Xu H, Zou L, Yang Q, Su X, Peng L and Jiao B. NEAT1 is required for survival of breast cancer cells through FUS and miR-548. *Gene Regul Syst Bio* 2016; 10: 11-17.